ACS Catalysis

pubs.acs.org/acscatalysis
Research Article

Spectroscopic Evidence of a Reduced Alkenylnickel Intermediate in Catalytic Markovnikov-Selective Alkyne Hydroboration

Jeong Woo Lee,[§] Gun Ha Kim,[§] Seo Yeong Jeong,[§] Ji Hwan Jeon, Hyejin Kwon, Yung Sam Kim, Byunghyuck Jung, Sangwon Seo, Jan-Uwe Rohde,* and Sung You Hong*

Cite This: ACS Catal. 2026, 16, 7551−7561
Read Online

ACCESS | Metrics & More | Article Recommendations | Supporting Information

ABSTRACT: Nickel-catalyzed hydrofunctionalization reactions, including the hydroboration of alkynes, have been generally proposed to proceed via classical two-electron pathways or, alternatively, through a $Ni^{I}H$-based insertion mechanism. Despite efforts to discern these pathways, explicit spectroscopic observation of $Ni^{I}H$ species and relevant mechanistic information on LNi^{I}(alkenyl) species remain lacking. Herein, we provide experimental evidence of formal Ni^{I} intermediates, suggestive of a $Ni^{I}H$-based insertion mechanism for alkyne hydroboration. The formation of a Ni^{I} catalyst precursor, L_nNi^{I}(dpm) (dpm = dipivaloylmethanate anion) and an L_nNi(alkenyl) intermediate was confirmed by EPR spectroscopy and HRMS analysis. Their involvement in the catalytic reaction was demonstrated by stoichiometric and catalytic reactivity studies. The origin of the counterintuitive Markovnikov selectivity in the formation of the α-alkenylboronate product was probed by systematic ligand electronic effect studies. Computational analyses rationalize the selectivity by a kinetic preference for formation of the α regioisomer of the L_nNi(alkenyl) intermediate through noncovalent interactions.

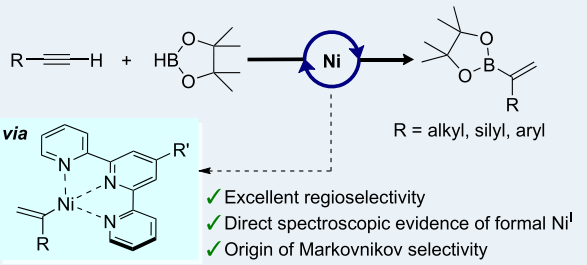

KEYWORDS: *alkenylboronates, EPR spectroscopy, hydroboration, Markovnikov selectivity, mechanistic study, nickel(I)*

1. INTRODUCTION

Nickel-catalyzed hydrofunctionalization of unsaturated systems has received significant attention, not merely as a low-cost alternative to reactions using precious metals, including Pd and Pt, but because Ni offers unique reactivity patterns: access to radical cascade pathways by facile single-electron transfer (SET),[1−3] slower β-hydrogen elimination,[2,4] and facile activation of diverse bonds that enables new possibilities for bond construction.[5,6] A key challenge in nickel-catalyzed hydrofunctionalization is the limited mechanistic understanding. Nickel-catalyzed hydrofunctionalization reactions have been generally proposed to proceed either through classical two-electron organometallic pathways involving oxidative addition, hydrometalation, and reductive elimination, or alternatively through a $Ni^{I}H$-based insertion mechanism (Scheme 1A). Despite computational studies considering NiH or Ni(alkenyl) complexes as catalytic intermediates, unambiguous elucidation of reaction pathways through characterization of catalytic intermediates remains relatively lacking.[7−17] Given our interest in developing nickel-catalyzed reactions and identifying key intermediates,[18−23] we decided to investigate whether nickel catalysis can promote the hydroboration of terminal alkynes, enabling access to alkenylboronates, an important class of organoboron compounds widely used in the synthesis of substituted olefins,[24−32] while also allowing characterization of key catalytic intermediates.

For the synthesis of alkenylboronates, both stoichiometric[26,27] and catalytic[28−32] hydroboration reactions of alkynes have emerged as a valuable synthetic strategy. However, such transformations have been largely restricted to the formation of β-alkenylboronates because of the intrinsic kinetic and thermodynamic preferences for anti-Markovnikov selectivity. To overcome these preferences and access the branched regioisomers, a copper-catalyzed protoboration approach has been established employing diboron reagents in conjunction with an external proton source.[32−40] Despite these advances, protoboration inevitably entails the use of a diboron moiety, consumes one boronate equivalent giving a stoichiometric byproduct in the formation of the desired products, and requires an additional proton source. To address these limitations, Markovnikov-selective catalytic hydroboration of alkynes has gained attention as an atom-economic alternative to protoboration. Recent studies have reported several methods for the Markovnikov hydroboration of terminal alkynes, yielding α-alkenylboronates.[41−45] For instance, Gade and Lu independently developed methods for cobalt-catalyzed

Received: January 6, 2026
Revised: March 20, 2026
Accepted: March 23, 2026
Published: April 8, 2026

https://doi.org/10.1021/acscatal.6c00028
ACS Catal. 2026, 16, 7551−7561

Scheme 1. Challenges in Nickel-Catalyzed Hydrofunctionalization

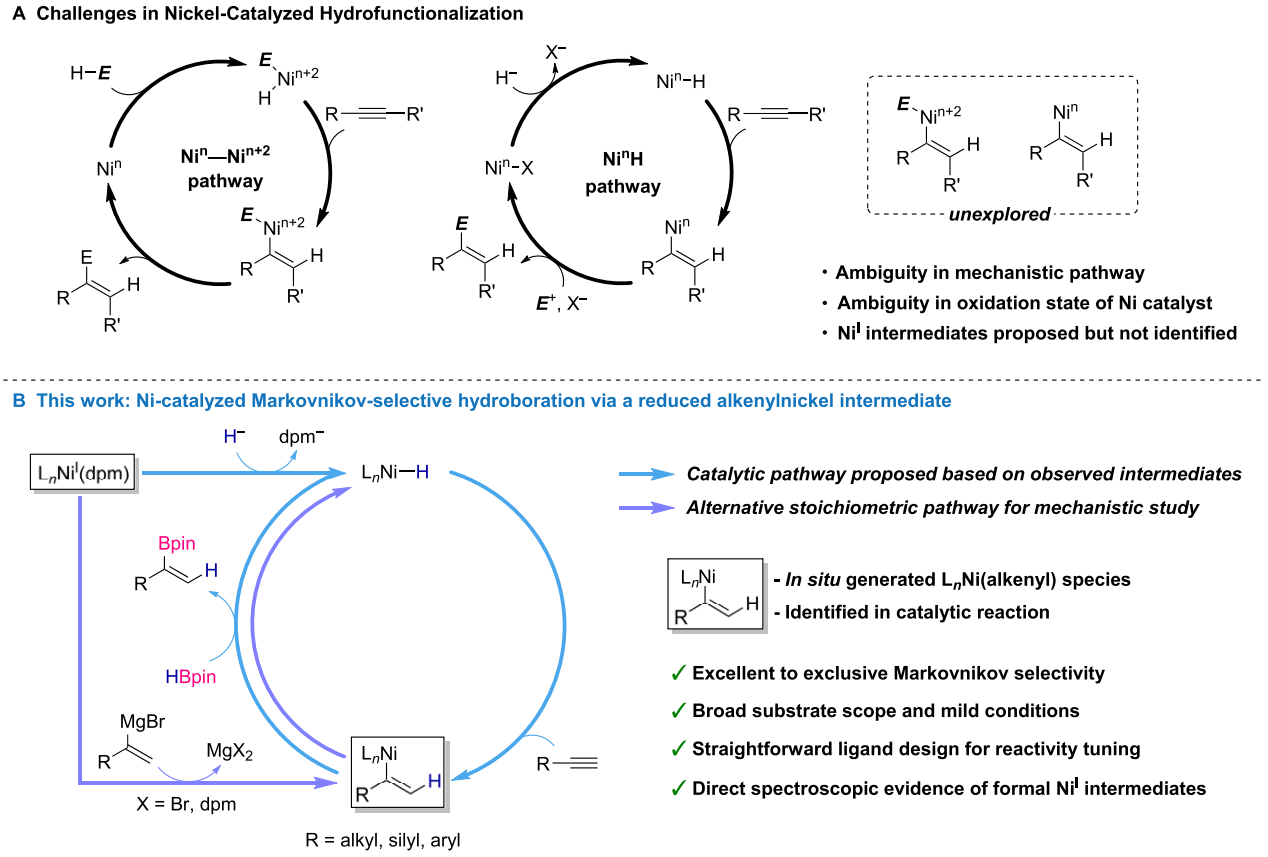

hydroboration of aryl-substituted terminal alkynes with pinacolborane (HBpin).[42,43] Nevertheless, universally applicable Markovnikov-selective hydroboration methods remain rare due to the intrinsic preference for anti-Markovnikov selectivity.

Herein, we report a Markovnikov-selective hydroboration of terminal alkynes using HBpin and a nickel catalyst supported by a substituted terpyridine ligand (Scheme 1B). The reaction is amenable to a broad range of alkynes, giving α-alkenylboronates with excellent regioselectivity under mild reaction conditions. Synthetic applications of the α-alkenylboronates are also examined. This work provides direct spectroscopic evidence for the involvement of two formal Ni^I complexes, $L_nNi^I(dpm)$ and $L_nNi(alkenyl)$, in the catalytic reaction, suggesting the intermediacy of an L_nNi^IH species in the catalytic cycle. The alkenylnickel intermediate was independently generated and, in reaction with HBpin, afforded the same product as the catalytic reaction. In addition, isotopic labeling experiments support a *syn* hydronickelation pathway in which HBpin serves as the major hydride source, while indicating a mechanism distinct from that previously reported for cobalt-catalyzed hydroboration. The origin of the Markovnikov selectivity was elucidated through combined experimental and computational investigations.

2. RESULTS AND DISCUSSION

2.1. Optimization of Reaction Conditions

We initiated our investigation of nickel-catalyzed hydroboration using dodec-1-yne (**1a**) as a model substrate of unactivated aliphatic terminal alkynes and HBpin as a reaction partner. After judicious evaluation of precatalysts, ligands, and additives (Supporting Information, Section II), the reaction conditions were optimized using $Ni(dpm)_2$ as a precatalyst and terpyridine **L1** as a ligand in THF, giving α-alkenylboronate **2a** with excellent Markovnikov selectivity and in 77% isolated yield (Table 1, entry 1). In the absence of $Ni(dpm)_2$, hydroboration products **2a** and **3a** were hardly found (entry 2). The use of $Ni(acac)_2$ or $Ni(cod)_2$ instead of $Ni(dpm)_2$ gave diminished yields of **2a** (entries 3 and 4). Without the additive $NiCl_2$·dme, the yield and regioselectivity were also decreased (entry 5). However, using 10 mol % NH_4Cl instead afforded a yield and regioselectivity comparable with those obtained under the optimized conditions (entry 6). Interestingly, the use of an NNN pincer ligand like **L1** was essential to form branched **2a** (entries 7, 12, and 13), as the absence of a ligand (entry 7) or the use of other ligands, such as diphosphine **L5** or bipyridine **L6** (entries 12 and 13), resulted in negligible yields or reversed regioselectivity. A lower loading of **L1** led to inferior performance (entry 8). Notably, the substituent on the central pyridine ring of the terpyridyl ligand significantly influenced both yield and regioselectivity (entries 9−11). For instance, the use of *p*-chloro-substituted terpyridine **L3** failed to afford the α-alkenylboronate (entry 10). These results revealed the importance of an electronically adjusted terpyridyl framework for this regioselective catalytic hydroboration.

2.2. Reaction Scope

With the optimized conditions in hand, we evaluated the generality of this transformation as illustrated in Scheme 2. An array of simple alkyl- and cycloalkyl-substituted terminal alkynes smoothly underwent the catalytic hydroboration with excellent Markovnikov selectivity (regioisomeric ratio, **2**:**3**, up to rr >99:1) to furnish α-alkenylboronates (**2a**−**2f**) in isolated

https://doi.org/10.1021/acscatal.6c00028
ACS Catal. 2026, 16, 7551−7561

Table 1. Optimization of Reaction Conditions[a]

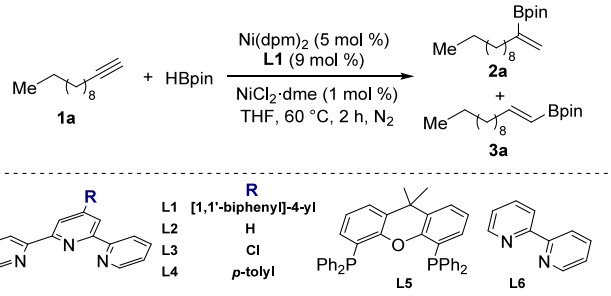

entry	deviation from standard conditions	yield of **2a** (%)	rr (**2a**:**3a**)
1	none	81 (77)	95:5
2	w/o $Ni(dpm)_2$	<1	-
3	$Ni(acac)_2$ instead of $Ni(dpm)_2$	62	92:8
4	$Ni(cod)_2$ instead of $Ni(dpm)_2$	52	96:4
5	w/o $NiCl_2$·dme	51	86:14
6[b]	NH_4Cl instead of $NiCl_2$·dme	76	96:4
7	w/o **L1**	<1	-
8	6 mol % of **L1**	47	89:11
9	**L2** instead of **L1**	27	73:27
10	**L3** instead of **L1**	n.d.	-
11	**L4** instead of **L1**	61	94:6
12	**L5** instead of **L1**	7	<1:99
13	**L6** instead of **L1**	n.d.	-

[a]Standard conditions: **1a** (0.40 mmol), HBpin (0.48 mmol, 1.2 equiv), $Ni(dpm)_2$ (5 mol %), **L1** (9 mol %), $NiCl_2$·dme (1 mol %) in THF (2 mL) at 60 °C for 2 h under an N_2 atmosphere. dpm = dipivaloylmethanate or 2,2,6,6-tetramethyl-3,5-heptanedionate, dme = 1,2-dimethoxyethane. Yield and regioisomeric ratio (rr) were determined by ^{1}H NMR analysis using TMSPh as an internal standard. TMSPh = phenyltrimethylsilane. Isolated yield is given in parentheses. [b]10 mol % NH_4Cl was used.

yields of 71−83%. This protocol was also suitable for a gram-scale synthesis giving **2a** in 70% isolated yield (see the SI, Section III, for the detailed procedure). A broad range of functional groups, including chloro (**2g**, **2h**), cyano (**2i**) and ester (**2j**, **2k**) groups, remained intact. Phthalimide (**2l**, **2m**), silyl ether (**2n**) and sulfonate ester (**2o**) groups were also compatible with this protocol. Remarkably, this method could be expanded to an array of silyl-substituted alkynes to furnish *gem*-borylsilyl alkenes (**2p**−**2t**) with exclusive Markovnikov selectivity in good isolated yields.

We further explored the reaction scope by using aryl-substituted alkynes. Remarkably, α-alkenylboronates were exclusively obtained regardless of the aryl substitution pattern. Methyl (**2u**), methoxy (**2v**), bromo (**2w**), fluoro (**2x**), trifluoromethyl (**2y**), trifluoromethoxy (**2z**), ester (**2aa**), cyano (**2ab**), and methylthio (**2ac**) groups in *ortho* position were tolerated and gave the corresponding products in moderate to good yields. Phenyl-substituted alkynes lacking *ortho* substituents gave further-hydrogenated side products **4** (Scheme S2); thus HBpin was used as the limiting reactant in these cases (**2ad**−**2ak**). Di- and trisubstituted aryl alkynes afforded **2al**−**2an** in 85−90% isolated yields. Heteroaromatic substrates, including 3-ethynylpyridine and Boc- or Me-protected 3-ethynylindoles, underwent the reaction to furnish the corresponding α-alkenylboronates (**2ao**−**2aq**). Naphthyl-, phenanthryl-, and pyrenyl-substituted alkynes were suitable for this catalytic hydroboration (**2ar**−**2at**), as well. While **2** could be isolated in all cases, except for **2z** and **2ab**, quantification of **4** was not feasible for every substrate due to signal overlap in the NMR spectra, and isolation of **3** and **4** was further limited by purification difficulties.

To evaluate the synthetic utility of this hydroboration, we leveraged the structural features of 1,1-borylsilylalkenes, which offer the potential for orthogonal functionalization at two distinct metalloid moieties, thereby enabling access to a variety of 1,1-difunctionalized olefins. As a representative example, bexarotene (Targretin), an anticancer drug, was synthesized via sequential cross-coupling reactions (Scheme 3A). In addition, one-pot modification of the substituted propargylamine known as pargyline through catalytic hydroboration and subsequent arylation was demonstrated (Scheme 3B).

2.3. Initial Mechanistic Studies

Having explored the efficacy of the Markovnikov-selective catalytic hydroboration reaction, we shifted our attention to the identification of the active catalytic species. Given the reductive conditions of this reaction system, we surmised that low-valent Ni species, including formal Ni^I complexes, or organic radical species may be involved as intermediates. To investigate the presence of organic radical intermediates, the catalytic reaction was conducted in the presence of 1,1-diphenylethylene, a commonly used radical inhibitor,[46−49] and the reaction proceeded smoothly (78%, Scheme 4A). By contrast, the use of TEMPO completely shut down the catalytic reaction, albeit TEMPO adducts, such as an alkenyl-TEMPO adduct (SI, Figure S1), were not detected. It is possible that TEMPO deactivated the active Ni catalyst,[7,50−52] presumably a reduced Ni species, such as a Ni^I, $Ni^{II}(L^{\bullet-})$, or Ni^0 species. Moreover, given that substrate **1d**, bearing a cyclopropyl group frequently used as a radical probe, smoothly afforded **2d** as the major product without ring opening, these observations are inconsistent with a radical-mediated pathway.

Based on these observations and our use of the precatalyst $Ni(dpm)_2$/**L1** under reducing conditions (HBpin), we considered the formation of $Ni^I(dpm)$(**L1**) (**5**) as a possible precursor complex and decided to evaluate its role in the catalytic reaction. This complex could be generated by comproportionation of $Ni(dpm)_2$ and $Ni(cod)_2$ in the presence of **L1** (see Section 2.4 for the characterization of this complex). When **5**, generated in situ, was used in place of $Ni(dpm)_2$ in the catalytic hydroboration reaction of **1a** (Scheme 4B), **2a** was obtained in a yield indistinguishable from that under standard conditions (77%, isolated yield).

2.4. Characterization and Reactions of Catalytic Ni Intermediates

Encouraged by the high catalytic activity of **5**, we set out to investigate the presence of formal Ni^I complexes in the catalytic reaction by EPR spectroscopy. To establish a suitable time frame for this purpose, we monitored the conversion of alkyne **1a** into alkenylboronate **2a** using ^{1}H NMR spectroscopy (SI, Figure S2). At t = 30 min, the reaction had progressed substantially but had not yet been completed. Thus, this time was deemed appropriate for the detection of reaction intermediates.

The EPR spectrum of a sample obtained from the standard reaction mixture (reaction I, 30 min) revealed two distinct resonance signals with g-factors of 2.198 and 1.9998 (Figure 1, black line). The g = 2.198 signal was assigned to $Ni^I(dpm)$-(**L1**) (**5**) based on comparison with the EPR spectrum of a sample of **5** obtained from the comproportionation reaction (Scheme 4B), showing a resonance signal with identical

https://doi.org/10.1021/acscatal.6c00028
ACS Catal. 2026, 16, 7551−7561

Scheme 2. Substrate Scope of Markovnikov-Selective Hydroboration Reactions[a]

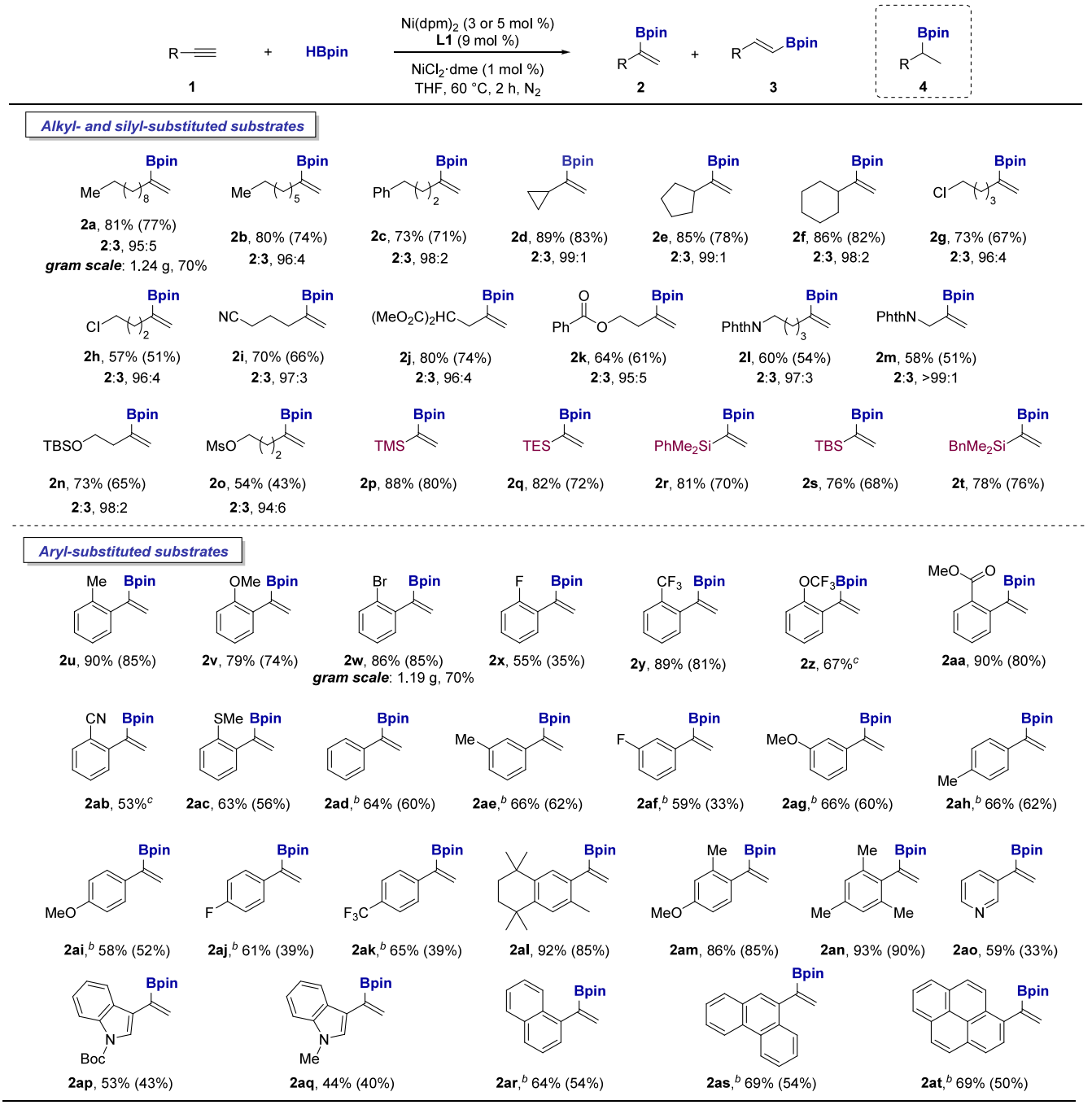

[a]Standard conditions: **1** (0.40 mmol), HBpin (0.48 mmol, 1.2 equiv), $Ni(dpm)_2$ (3 or 5 mol %), **L1** (9 mol %), $NiCl_2$·dme (1 mol %) in THF (2 mL) at 60 °C for 2 h under an N_2 atmosphere. Yields of **2** and regioisomeric ratios (**2**:**3**) were determined by ^1H NMR analysis of the crude products using TMSPh as an internal standard. Isolated yields of **2** are given in parentheses. Phth = phthaloyl, TBS = *t*-butyldimethylsilyl, Ms = mesyl or methanesulfonyl, TMS = trimethylsilyl, TES = triethylsilyl. [b]Reaction conditions: **1** (0.60 mmol), HBpin (0.40 mmol), $Ni(dpm)_2$ (3 or 5 mol %), **L1** (9 mol %), $NiCl_2$·dme (1 mol %) in THF (2 mL) at 60 °C for 2 h under an N_2 atmosphere. [c]Inseparable mixture, the ratio of **2**:**4** was determined by ^1H NMR analysis (SI, Section IV).

parameters (Figure 1, blue line). A similar signal with $g = 2.139$ was reported for the related complex $Ni^IBr(tpy)$ measured in DMF solution at room temperature.[53] This complex was synthesized in the same manner as **5** and characterized crystallographically. By contrast, $Ni(CH_3)(tpy)$ was characterized by a signal at $g = 2.021$ (THF, room temperature), which was attributed to a Ni^{II}-ligand-radical species.[54] Thus, the *g*-factor and peak-to-peak separation found here for **5** indicate that the unpaired electron spin density resides to a significant extent in a metal-based orbital. Depending on the bonding mode of the anionic dpm^- ligand, i.e., monodentate or bidentate, the Ni center may be either four-coordinate or five-coordinate and the complex either a 17-electron or a 19-electron species. Quantitation of **5** generated by comproportionation revealed that the accumulation of this complex was 93% under these conditions (SI, Section VII). Interestingly,

https://doi.org/10.1021/acscatal.6c00028
ACS Catal. 2026, 16, 7551−7561

Scheme 3. Synthetic Utility of Markovnikov-Selective Hydroboration

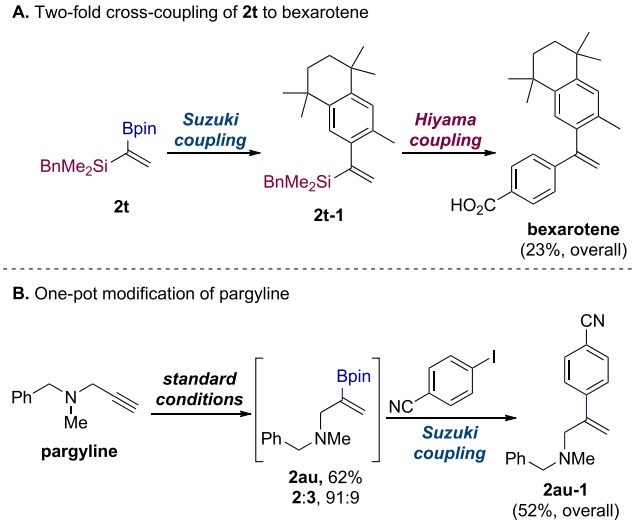

Scheme 4. Preliminary Mechanistic Investigation

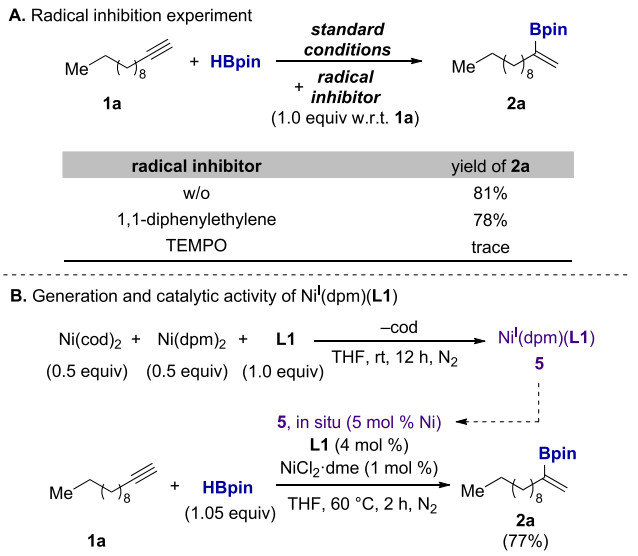

radical inhibitor	yield of **2a**
w/o	81%
1,1-diphenylethylene	78%
TEMPO	trace

the EPR spectrum of a sample of the catalytic hydroboration of **1a** using **5** formed in situ (Scheme 4B, t = 30 min) showed the same resonance signals as those found for reaction I but with greater intensities (SI, Figure S4, reaction II).

The formulation of **5** was corroborated by high-resolution mass spectrometry (HRMS). The mass spectrum of a sample of **5** obtained from the comproportionation reaction showed two peaks with the masses and isotope distribution patterns expected for $[Ni^{II}(dpm)(\mathbf{L1})]^+$ and $[Ni^{I}(\mathbf{L1})]^+$ (m/z = 626 and 443). These peaks are related to **5** by one-electron oxidation and loss of the dpm^- anion, respectively (SI, Figures S10 and S11). The substantially different intensities of these two features suggest that one-electron oxidation of **5** is more facile than dpm^- ligand dissociation (Figure S9).

For further investigation into the origin of the second EPR signal at g = 1.9998 (**6**), we carried out reaction I with different concentrations of alkyne **1a**. The EPR spectra of samples of these reactions revealed changes in the intensities of both resonance signals (Figure 2). When the concentration of **1a**

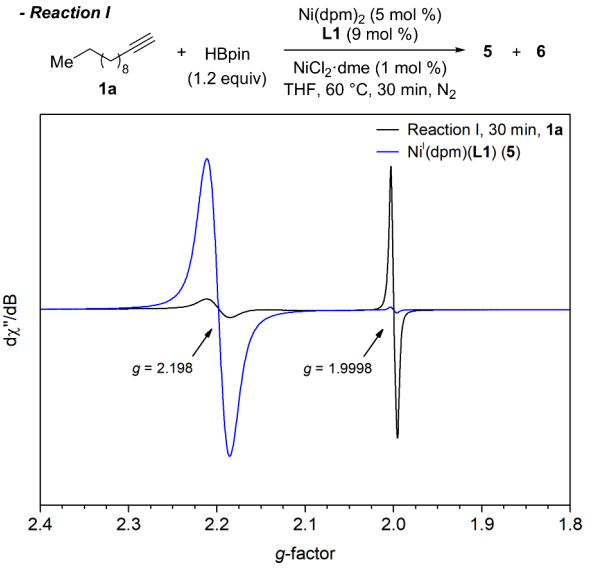

Figure 1. EPR spectra (X-band, 293 K) of a sample from the catalytic hydroboration of **1a** under standard conditions (reaction I, black line) and a sample of **5** generated by comproportionation (THF, 10 mM Ni, blue line). The small signal at g = 2.0003 in the spectrum of **5** was attributed to an impurity (SI, Figure S3).

was increased from 1 to 20 to 40 equiv w.r.t. $Ni(dpm)_2$, the signal intensity of **5** decreased, whereas that of **6** increased.

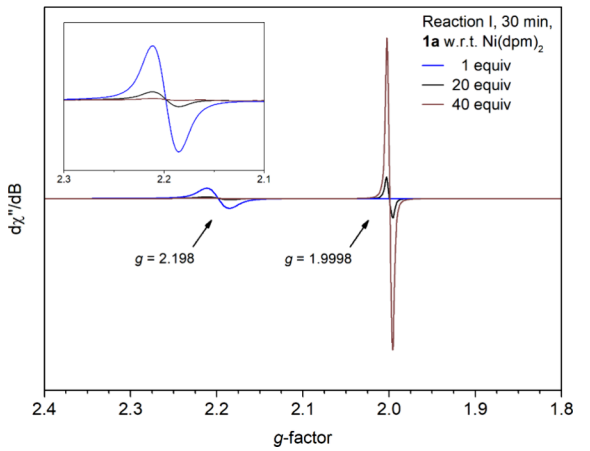

Figure 2. EPR spectra (X-band, 293 K) of samples from the catalytic hydroboration under standard conditions (reaction I) using varying amounts of alkyne **1a**: 1 equiv w.r.t. $Ni(dpm)_2$ (blue line), 20 equiv (black line), and 40 equiv (brown line). Inset: expanded view of the g = 2.2 region.

Suspecting that **6** could be a Ni complex derived from the alkyne substrate, we investigated reaction I with different alkynes to probe whether the identity of the alkyne employed affected the signal of **6**. In addition to **1a**, we used **1d**, **1p**, and **1ad**, representing cycloalkyl-, silyl-, and aryl-substituted alkynes. Indeed, while the spectra of each of these reactions exhibit the same pattern featuring the two resonance signals of **5** and **6**, a small shift could be discerned in the g-factor of **6** (SI, Figures S6 and S7 and Table S6). To determine the g-factors of these complexes with sufficiently high precision, the spectra were measured after calibration with a reference standard having a signal in this region (SI, Section VII).

https://doi.org/10.1021/acscatal.6c00028
ACS Catal. 2026, 16, 7551−7561

In addition, the high-resolution mass spectra of these reaction mixtures each showed a peak having the mass and isotope distribution pattern expected for the respective $[Ni^{II}(alkenyl)(\mathbf{L1})]^+$ ion (SI, Figures S12−S15). These ions could have arisen from one-electron oxidation of the corresponding Ni(alkenyl)(**L1**) complexes. Thus, the second resonance signal observed in each of the EPR spectra was assigned to Ni(dodecenyl)(**L1**) (**6a**), Ni(cyclopropylvinyl)-(**L1**) (**6d**), Ni(trimethylsilylvinyl)(**L1**) (**6p**), or Ni(styryl)-(**L1**) (**6ad**), respectively. Given that the major or exclusive products in the catalytic reactions are the α-alkenylboronates, the alkenyl complexes **6** may predominantly be the α regioisomers.

The electronic structure of alkenyl complexes **6** may be interpreted by a combination of a Ni^{I} and a Ni^{II}-ligand-radical configuration. While the resonance signals of **6**, having a peak-to-peak separation of 10−13 G, are broader than those of typical organic radicals, they are much narrower than the signal of **5**. Thus, the spectral parameters of **6** may suggest a dominant contribution from a Ni^{II}-ligand-radical configuration, presumably with significant Ni(3d) − L(π^*) mixing.

To confirm our assignment of **6**, we sought to generate one such complex independently. Because the corresponding Grignard reagent of **1ad**, α-styrylmagnesium bromide, is known, we pursued the preparation of **6ad** from **5** by transmetalation (Scheme 5A). Upon addition of 1.0 equiv of

Scheme 5. Generation and Stoichiometric Reaction of Ni(styryl)(L1) (6ad)

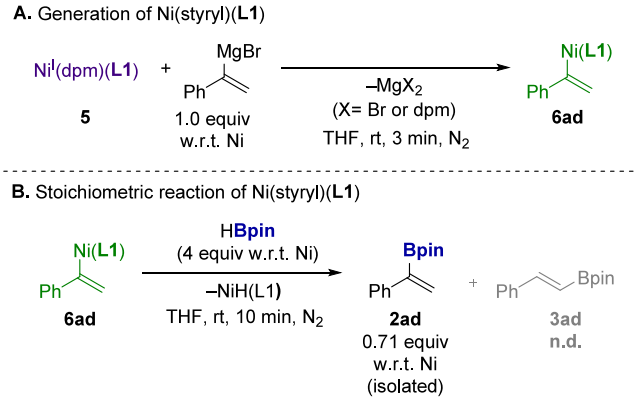

the Grignard reagent in THF (SI, Section VI.D) to a solution of **5**, the dark blue solution immediately turned dark green. The EPR spectrum of a sample of the reaction mixture at t = 3 min showed only the signal at g = 1.9996 (Figure 3, green line). This g-factor is indeed the same as the one observed for the standard reaction mixture prepared using **1ad** (t = 30 min). The signal of **5** was not observed. Quantitation of **6ad** generated in this manner revealed an accumulation of 72% (SI, Section VII). Furthermore, the presence of **6ad** in this reaction mixture was confirmed by HRMS, showing the same feature and m/z value as found for reaction I using **1ad.**

We then tested whether independently generated **6ad** can react with HBpin to release **2ad**. Reaction of **6ad** (t = 3 min) with 4 equiv of HBpin at room temperature (t = 10 min) afforded 0.71 equiv of **2ad** w.r.t. Ni, while no formation of **3ad** was observed (Scheme 5B and SI, Section VI.E). Thus, the reaction of **6ad** with HBpin can stoichiometrically provide the branched product. Moreover, given that only **2ad** was observed and no **3ad**, alkenylnickel complex **6ad** is presumably the α

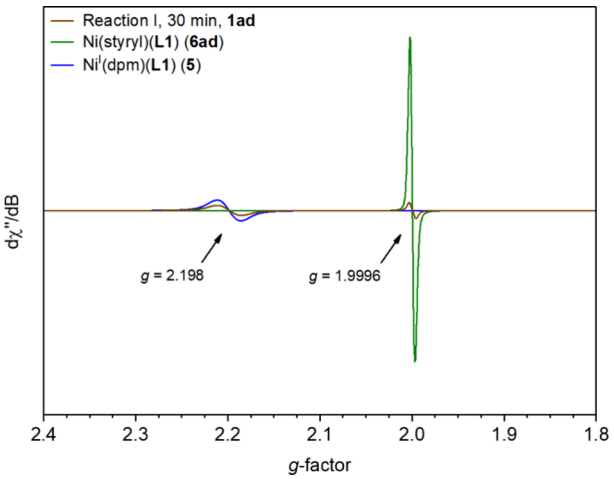

Figure 3. EPR spectra (X-band, 293 K) of a sample from the catalytic hydroboration of **1ad** under standard conditions (reaction I, brown line), a sample of **6ad** generated by transmetalation (THF, 10 mM Ni, green line), and a sample of **5** generated by comproportionation (THF, 10 mM Ni, blue line).

regioisomer. The Ni product in this reaction step may then be a hydridonickel complex, such as NiH(**L1**) (SI, Scheme S6).

2.5. Proposed Mechanism

Collectively, our investigations show that Ni^{I}(dpm)(**L1**) (**5**) and Ni(α-alkenyl)(**L1**) (**6**) are intermediates in this catalysis, while **5** and **6ad** were also characterized independently in stoichiometric reactions. On this basis, we hypothesized that during catalysis **5** reacts with HBpin and generates a nickel hydride complex, $Ni^{I}H$(**L1**), which adds to the alkyne and generates **6** (Scheme 6A). Based on this hypothesis, we performed deuterium-labeling experiments (Scheme 6B) to elucidate the formation pathway of the desired compound, with the alternate use of deuterium sources (i.e., **1c**-*d*/HBpin and **1c**/DBpin). The hydroboration of deuterium-labeled alkyne **1c**-*d* with HBpin under standard conditions gave (*Z*)-**2c**-*d* with 85% incorporation of D, as determined by ^{1}H NMR analysis. Conversely, the reaction of **1c** with DBpin (*ca.* 95 atom % D) led to (*E*)-**2c**-*d* with 85% incorporation of D. The isolation of these labeled *syn* addition products demonstrates that HBpin is the major hydride source and that it adds predominantly *syn* to the alkyne to afford the branched product. This experimental outcome is distinct from the H/D scrambling pathways previously reported for cobalt-catalyzed hydroboration reactions, where such scrambling was attributed to reversible Co−H-based alkyne insertion/β-hydrogen elimination events or to an Ojima−Crabtree-type rearrangement.[42,43] Combined with the observation of **5** and **6** by EPR spectroscopy, the results of the deuterium labeling experiments are consistent with the formation of $Ni^{I}H$(**L1**), which may undergo *syn*-selective hydronickelation of the alkyne to form α-alkenylnickel **6** (Scheme 6A).

Based on our experimental findings, a plausible mechanism for the nickel-catalyzed Markovnikov-selective hydroboration is proposed in Scheme 6C. The reaction of precatalyst Ni(dpm)$_2$/**L1** and HBpin affords the precursor complex **5**, which further reacts with HBpin to generate $Ni^{I}H$(**L1**) (**A**). Addition of **A** to terminal alkyne **1** gives π complex **B**. Subsequent migratory insertion of the terminal alkyne affords (α-alkenyl)nickel complex **6**. This intermediate, in turn, undergoes σ-bond metathesis with HBpin via the generation

https://doi.org/10.1021/acscatal.6c00028
ACS Catal. 2026, 16, 7551−7561

Scheme 6. Additional Mechanistic Studies and Proposed Reaction Mechanism

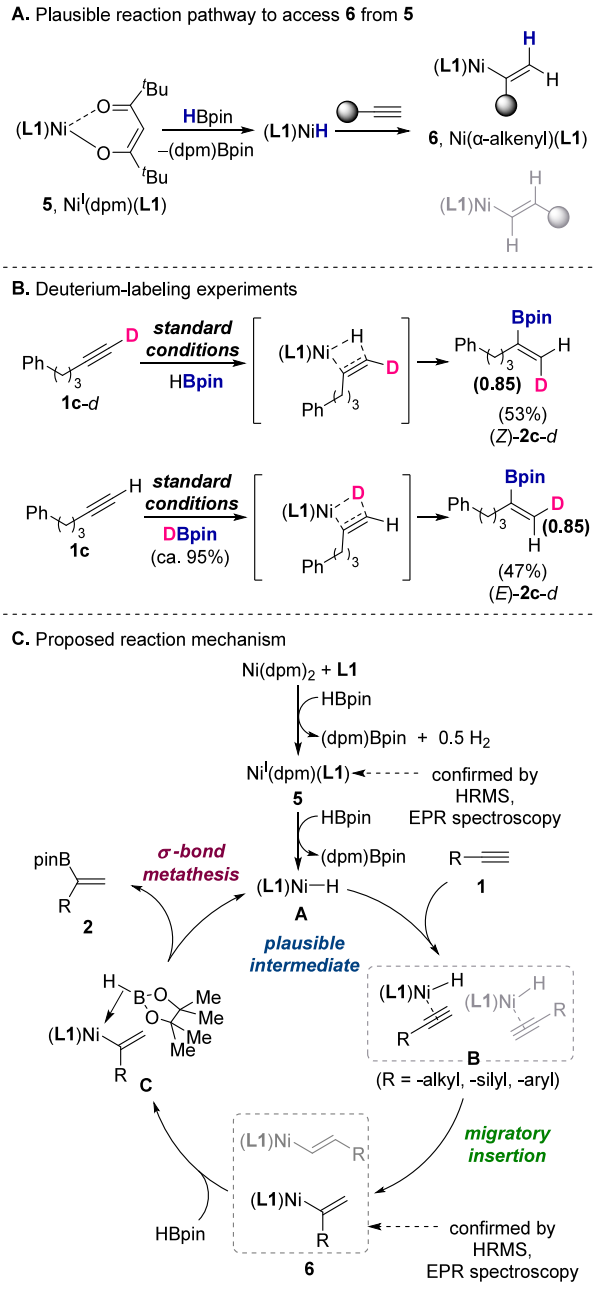

of σ complex **C** to produce α-alkenylboronate **2** and regenerate **A**. Although the role of the additive, $NiCl_2$·dme or NH_4Cl, is not clear at this stage of our investigation, it is conceivable that chloride affects the formation or stability of one of the Ni intermediates **A**, **B** or **6**.

2.6. Origin of Markovnikov Selectivity

To gain insight into the unconventional regioselectivity observed in this hydroboration, natural bond orbital (NBO) charges were calculated to compare the charge distribution across the C(sp)−C(sp) triple bond of the alkyne quantitatively (Table 2A) and to evaluate the possible influence of substrate electronics on the regioselectivity. For substrate **1p**, bearing an electron-donating silyl group, the charge on C(α) was found to be more negative than that on C(β). This charge difference could direct hydronickelation in a Markovnikov-selective pathway through polarity alignment with the L_nNiH species, which consistently exhibits a negative charge on the H atom and a positive charge on the Ni atom. The formation of the α-alkenylboronate (**2p**) is plausible based on this calculation and consistent with our experimental results showing the absence of β-alkenylboronates **3** in reactions involving silyl-substituted alkynes. For other substrates such as **1a**, **1d** and **1f**, however, the charge on C(α) is more positive than that on C(β), and polarity alignment between these alkynes and L_nNiH contradicts the observed Markovnikov selectivity. These results suggest that the electronic nature of the alkyne substrates is unlikely to be the dominant factor governing our Markovnikov-selective hydroboration.

To assess the influence of ligand electronics on the selectivity experimentally, we examined the hydroboration reactions of the aforementioned representative substrates using three electronically distinct terpyridine ligands (Table 2B). This approach was prompted by our optimization study, which showed that both regioselectivity and yield are considerably influenced by the substituent in 4′-position of the ligand (see Table 1, entries 1 and 8−10). We tested the unsubstituted terpyridine (**L2**) and terpyridine ligands with an electron-donating or an electron-withdrawing substituent installed in 4′-position (**L7** or **L8**).

Indeed, the electronic nature of the substituent considerably affected both yield and regioselectivity. The ligand bearing an electron-donating dimethylamino group (**L8**) led to substantially reduced yields and reversed selectivity (7%, rr = 32:68, for **1a**; Table 2B), as observed across the alkynes. In sharp contrast, an electron-withdrawing cyano-substituted terpyridine ligand (**L7**) delivered markedly improved yields and regioselectivity (60%, rr = 97:3, for **1a**; Table 2B), comparable to those observed with the optimized ligand, **L1**. These findings indicate that the electronic nature of the ligand, and by extension that of the catalytic intermediate, directs the regioselectivity, rather than the simple polarity alignment between the substrate and the L_nNiH complex.

To gain more insight into the regiodetermining factors in this unusual Markovnikov-selective hydroboration, we conducted density functional theory (DFT) calculations based on the proposed Ni^I catalytic pathway (Figure 4). We selected the optimal terpyridine ligand **L1** and aliphatic alkyne **1b** as a model substrate for this investigation, as it is electronically unbiased, and because hydroboration of a series of aliphatic terminal alkynes has previously been shown to favor anti-Markovnikov addition.[55−58] In contrast to the reported systems, our calculations indicate that Markovnikov hydronickelation (**B-TS**) is kinetically favored over anti-Markovnikov hydronickelation (**B′-TS**) (Figure 4A, $\Delta\Delta G^{\ddagger}$ = 2.1 kcal/mol), consistent with the experimental observations (rr = 96:4). The formation of alkenylnickel intermediates **6b** and **6b′** is highly exergonic (ΔG = −22.5 kcal/mol and −22.8 kcal/mol, respectively), suggesting that the reverse reaction is unlikely and the hydronickelation is indeed the regiodetermining step.

Notably, the Markovnikov hydronickelation pathway also features a lower-energy Ni(alkyne) intermediate (**B′** vs **B**; $\Delta\Delta G$ = 2.4 kcal/mol). This result is counterintuitive, given that **B** is expected to be sterically less favored than **B′**. To obtain an energy profile of the hydronickelation step for each pathway, we performed distortion-interaction analysis (Figure 4B) as a form of energy decomposition analysis. We found that the distortion energy term is significantly lower for the

https://doi.org/10.1021/acscatal.6c00028
ACS Catal. 2026, 16, 7551−7561

Table 2. Investigations into Origin of Regioselectivity

A Calculated NBO charges[a]

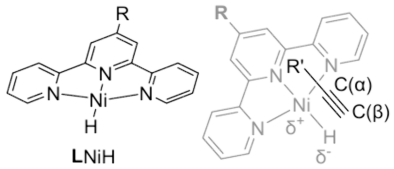

	R	Ni	H
L7	CN	0.320	−0.176
L2	H	0.297	−0.181
L8	NMe_2	0.244	−0.184

B Ligand substituent effect on the yield and the regioselectivity[b]

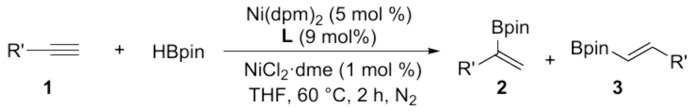

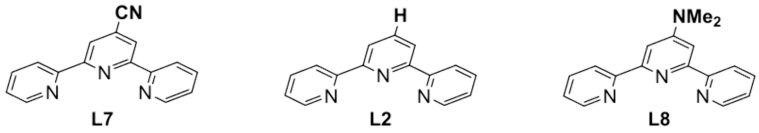

	R'	C(α)	C(β)	yield of **2** (%)	rr (**2**:**3**)	yield of **2** (%)	rr (**2**:**3**)	yield of **2** (%)	rr (**2**:**3**)
1a	*n*-$C_{10}H_{21}$	−0.004	−0.281	60	97:3	27	73:27	7	32:68
1d	*cyclo*-Pr	−0.013	−0.270	84	98:2	62	90:10	10	24:76
1f	Cy	0.004	−0.271	72	>99:1	74	88:12	10	41:59
1p	TMS	−0.499	−0.194	55	-	71	-	4	-

[a]NBO charges were calculated at the uM06/6−311+G**|SDD(Ni)/SMD(THF) level of theory with geometries optimized at the uB3LYP-D3/6−31G**|SDD(Ni) level. [b]Yields and regioisomeric ratios were determined by ^{1}H NMR analysis using TMSPh as an internal standard (confer Table 1).

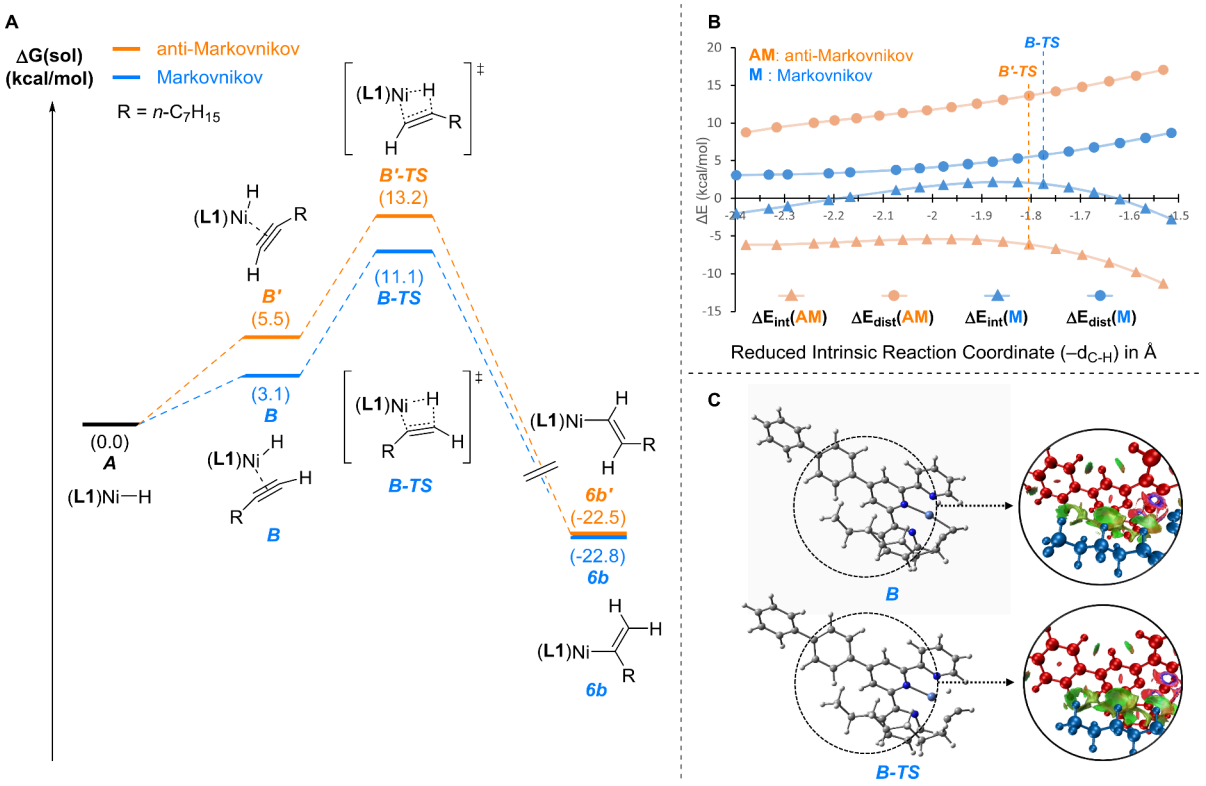

Figure 4. DFT calculations of the hydronickelation step of the proposed catalytic cycle. (A) Energy profile calculated at the uM06/6−311+G**|SDD(Ni)/SMD(THF) level of theory with geometries optimized at the uB3LYP-D3/6−31G**|SDD(Ni) level. (B) Distortion-interaction analysis along the reaction coordinate, obtained by plotting the relative electronic energy (*y*-axis) as a function of the negative value of the distance between the bond-forming C and H atoms (*x*-axis). (C) Calculated structures of **B** and **B-TS** and their NCI analysis.

https://doi.org/10.1021/acscatal.6c00028
ACS Catal. 2026, 16, 7551−7561

Markovnikov pathway ($\Delta E_{dist}(\mathbf{M})$) than for the anti-Markovnikov pathway ($\Delta E_{dist}(\mathbf{AM})$), which implies that the Markovnikov transition state requires less structural reorganization.

In line with these findings, the calculated structures of **B** and **B-TS** both exhibit alignment of the alkyl chain of the substrate with the central pyridine of the terpyridine ligand, and the distances between the centroid of this pyridine ring and the closest H atom of the alkyl chain were identified as 2.68 Å in **B** and 2.72 Å in **B-TS** (Figure S22A). To verify whether this alignment can arise from noncovalent interactions (NCIs), we conducted reduced density gradient (RDG) analysis[59] to investigate attractive interactions between the central pyridine and the C(sp^3)−H moieties. Indeed, weak attractive interactions were observed in both structures (visualized as green regions in Figure 4C, rendered using GaussView[60] and VMD[61], Figure S22). NCIs, such as these weak interactions, have been proposed as stabilizing factors that enhance selectivity in various catalytic systems.[62−65] In our system, the C−H···π interaction may cause the Ni(alkyne) coordination to energetically favor **B** over **B′**, while also stabilizing the Markovnikov transition state (**B-TS** over **B′-TS**, SI, Section XI, for further interpretation).

Overall, the unconventional Markovnikov selectivity observed in this catalytic system can be attributed to the electronic nature of the Ni intermediate tailored by substituents of the terpyridine ligand, as supported by the NBO analysis and the systematic experimental investigation of the ligand effect. DFT calculations on the hydronickelation step revealed that the structures of **B** and **B-TS** are lower in energy than their anti-Markovnikov counterparts, and distortion-interaction and NCI analyses suggest that the Markovnikov pathway requires less structural reorganization due to weak attractive C−H···π interactions between the ligand and the substrate (Figure 4).

3. CONCLUSION

In summary, we have demonstrated a Markovnikov-selective hydroboration of terminal alkynes to afford α-alkenylboronates under mild reaction conditions, while reversing the conventional anti-Markovnikov selectivity. The catalytic protocol is broadly applicable, exhibiting excellent Markovnikov selectivity across alkyl-, aryl-, and silyl-substituted alkynes. The synthetic utility of this method has been showcased through the facile synthesis of biologically active bexarotene and the derivatization of pargyline.

Although nickel-catalyzed hydrofunctionalization has shown remarkable progress, direct experimental identification of catalytically relevant nickel species remains scarce. The frequently proposed Ni^{I} and Ni^{II} intermediates have been debated, and most mechanistic hypotheses rely on computational chemistry in the absence of experimental evidence. In this work, mechanistic and spectroscopic studies revealed the formation of two formal Ni^{I} intermediates, Ni^{I}(dpm)(**L1**) and Ni(α-alkenyl)(**L1**), which were characterized by EPR spectroscopy and mass spectrometry. While Ni^{I}(dpm)(**L1**) was shown to be a precursor of Ni(alkenyl)(**L1**) under catalytic conditions, the latter could exclusively afford the corresponding α-alkenylboronate in the stoichiometric reaction with HBpin, indicating their intermediacy in this protocol.

Deuterium labeling studies revealed *syn* addition of HBpin to the terminal alkyne. This is consistent with *syn* hydronickelation of the terminal alkyne and indicates a stabilization mechanism distinct from that of cobalt-catalyzed systems. In addition, the terpyridine ligands employed in this study are readily accessible through concise synthetic sequences, in contrast to previously reported catalytic systems that rely on multistep ligand syntheses. A systematic investigation of ligand substituent effects on the reactivity across the tested alkyne substrates revealed that the regioselectivity and yield are primarily dominated by electronic properties of the ligand. Computational studies further suggested that noncovalent interactions between the substrate and the terpyridine ligand can contribute to the stabilization of the transition state along the Markovnikov-selective pathway. We anticipate that our method, together with the mechanistic insights on reduced Ni intermediates, will not only offer mild and efficient access to α-alkenylboronates but also expand the understanding of NiH-catalyzed hydrofunctionalization reactions.

METHODS

General Procedure for Markovnikov-Selective Hydroboration of Alkyne Substrates

In an N_2-filled glovebox, a 4 mL screw-cap vial containing a magnetic stir bar was charged with Ni(dpm)$_2$ (8.5 mg, 0.020 mmol, 5 mol %), **L1** (14 mg, 0.036 mmol, 9 mol %), $NiCl_2$·dme (0.9 mg, 0.004 mmol, 1 mol %), anhydrous THF (2.0 mL) and alkyne **1** (0.40 mmol, 1.0 equiv). The reaction mixture was stirred at rt for 1 min. Then, HBpin (70 μL, 62 mg, 0.48 mmol, 1.2 equiv) was added to the vial. After being sealed, the vial was taken out of the glovebox and the mixture was stirred at 60 °C for 2 h. The mixture was diluted with Et_2O, filtered through a syringe filter and the filtrate was concentrated in vacuo. The residue was purified by flash column chromatography on silica or by using a Biotage Isolera purification system to afford the corresponding α-alkenylboronate (see the Supporting Information for more details).

ASSOCIATED CONTENT

Supporting Information

The Supporting Information is available free of charge at https://pubs.acs.org/doi/10.1021/acscatal.6c00028.

Detailed experimental procedures, characterization data, and spectroscopic data (PDF)

AUTHOR INFORMATION

Corresponding Authors

Jan-Uwe Rohde − *Department of Chemistry, Ulsan National Institute of Science and Technology (UNIST), Ulsan 44919, Republic of Korea;* orcid.org/0000-0002-0691-6699; Email: rohde@unist.ac.kr

Sung You Hong − *Department of Chemistry, Ulsan National Institute of Science and Technology (UNIST), Ulsan 44919, Republic of Korea;* orcid.org/0000-0002-5785-4475; Email: syhong@unist.ac.kr

Authors

Jeong Woo Lee − *Department of Chemistry, Ulsan National Institute of Science and Technology (UNIST), Ulsan 44919, Republic of Korea*

Gun Ha Kim − *Department of Chemistry, Ulsan National Institute of Science and Technology (UNIST), Ulsan 44919, Republic of Korea*

Seo Yeong Jeong − *Department of Chemistry, Ulsan National Institute of Science and Technology (UNIST), Ulsan 44919, Republic of Korea*

https://doi.org/10.1021/acscatal.6c00028
ACS Catal. 2026, 16, 7551−7561

Ji Hwan Jeon − *Department of Chemistry, Ulsan National Institute of Science and Technology (UNIST), Ulsan 44919, Republic of Korea*

Hyejin Kwon − *Department of Chemistry, Ulsan National Institute of Science and Technology (UNIST), Ulsan 44919, Republic of Korea*

Yung Sam Kim − *Department of Chemistry, Ulsan National Institute of Science and Technology (UNIST), Ulsan 44919, Republic of Korea;* orcid.org/0000-0001-6306-7438

Byunghyuck Jung − *Department of Physics and Chemistry, Daegu Gyeongbuk Institute of Science and Technology (DGIST), Daegu 42988, Republic of Korea;* orcid.org/0000-0002-8582-082X

Sangwon Seo − *Department of Physics and Chemistry, Daegu Gyeongbuk Institute of Science and Technology (DGIST), Daegu 42988, Republic of Korea;* orcid.org/0000-0003-2281-9167

Complete contact information is available at: https://pubs.acs.org/10.1021/acscatal.6c00028

Author Contributions

[§]J.W.L., G.H.K., and S.Y.J. equally contributed to this work.

Notes

The authors declare no competing financial interest.

■ ACKNOWLEDGMENTS

This research was supported by the Basic Science Research Program through the National Research Foundation of Korea (NRF) funded by the Ministry of Education (RS-2023-NR076557). G.H.K. is grateful for a postdoctoral fellowship supported by the Basic Science Research Program through the National Research Foundation of Korea (NRF) funded by the Ministry of Education (RS-2024-00452066).

■ REFERENCES

(1) Dawson, G. A.; Spielvogel, E. H.; Diao, T. Nickel-Catalyzed Radical Mechanisms: Informing Cross-Coupling for Synthesizing Non-Canonical Biomolecules. *Acc. Chem. Res.* **2023**, *56*, 3640−3653.

(2) Diccianni, J. B.; Diao, T. Mechanisms of Nickel-Catalyzed Cross-Coupling Reactions. *Trends Chem.* **2019**, *1*, 830−844.

(3) Ehehalt, L. E.; Beleh, O. M.; Priest, I. C.; Mouat, J. M.; Olszewski, A. K.; Ahern, B. N.; Cruz, A. R.; Chi, B. K.; Castro, A. J.; Kang, K.; Wang, J.; Weix, D. J. Cross-Electrophile Coupling: Principles, Methods, and Applications in Synthesis. *Chem. Rev.* **2024**, *124*, 13397−13569.

(4) Tasker, S. Z.; Standley, E. A.; Jamison, T. F. Recent Advances in Homogeneous Nickel Catalysis. *Nature* **2014**, *509*, 299−309.

(5) Sun, X.-Y.; Yao, B.-Y.; Xuan, B.; Xiao, L.-J.; Zhou, Q.-L. Recent Advances in Nickel-Catalyzed Asymmetric Hydrofunctionalization of Alkenes. *Chem. Catal* **2022**, *2*, 3140−3162.

(6) Wang, Y.; He, Y.; Zhu, S. NiH-Catalyzed Functionalization of Remote and Proximal Olefins: New Reactions and Innovative Strategies. *Acc. Chem. Res.* **2022**, *55*, 3519−3536.

(7) Du, B.; Ouyang, Y.; Chen, Q.; Yu, W.-Y. Thioether-Directed NiH-Catalyzed Remote γ-C(sp^3)−H Hydroamidation of Alkenes by 1,4,2-Dioxazol-5-ones. *J. Am. Chem. Soc.* **2021**, *143*, 14962−14968.

(8) He, Y.; Cai, Y.; Zhu, S. Mild and Regioselective Benzylic C−H Functionalization: Ni-Catalyzed Reductive Arylation of Remote and Proximal Olefins. *J. Am. Chem. Soc.* **2017**, *139*, 1061−1064.

(9) Zhou, F.; Zhu, J.; Zhang, Y.; Zhu, S. NiH-Catalyzed Reductive Relay Hydroalkylation: A Strategy for the Remote C(sp^3)−H Alkylation of Alkenes. *Angew. Chem., Int. Ed.* **2018**, *57*, 4058−4062.

(10) Zhang, Y.; Xu, X.; Zhu, S. Nickel-Catalyzed Selective Migratory Hydrothiolation of Alkenes and Alkynes with Thiols. *Nat. Commun.* **2019**, *10*, 1752.

(11) Lyu, X.; Zhang, J.; Kim, D.; Seo, S.; Chang, S. Merging NiH Catalysis and Inner-Sphere Metal-Nitrenoid Transfer for Hydroamidation of Alkynes. *J. Am. Chem. Soc.* **2021**, *143*, 5867−5877.

(12) Lee, C.; Seo, H.; Jeon, J.; Hong, S. γ-Selective C(sp^3)−H Amination via Controlled Migratory Hydroamination. *Nat. Commun.* **2021**, *12*, 5657.

(13) Gao, Y.; Yang, S.; Huo, Y.; Chen, Q.; Li, X.; Hu, X.-Q. NiH-Catalyzed Hydroamination/Cyclization Cascade: Rapid Access to Quinolines. *ACS Catal.* **2021**, *11*, 7772−7779.

(14) Wang, X.-X.; Xu, Y.-T.; Zhang, Z.-L.; Lu, X.; Fu, Y. NiH-Catalyzed Proximal-Selective Hydroalkylation of Unactivated Alkenes and the Ligand Effects on Regioselectivity. *Nat. Commun.* **2022**, *13*, 1890.

(15) Lee, C.; Kang, H.-J.; Seo, H.; Hong, S. Nickel-Catalyzed Regio- and Enantioselective Hydroamination of Unactivated Alkenes Using Carbonyl Directing Groups. *J. Am. Chem. Soc.* **2022**, *144*, 9091−9100.

(16) Zhang, Z.; Bera, S.; Fan, C.; Hu, X. Streamlined Alkylation via Nickel-Hydride-Catalyzed Hydrocarbonation of Alkenes. *J. Am. Chem. Soc.* **2022**, *144*, 7015−7029.

(17) Bera, S.; Fan, C.; Hu, X. Enantio- and Diastereoselective Construction of Vicinal C(sp^3) Centers via Nickel-Catalyzed Hydroalkylation of Alkenes. *Nat. Catal.* **2022**, *5*, 1180−1187.

(18) Kim, W. G.; Kang, M. E.; Lee, J. B.; Jeon, M. H.; Lee, S.; Lee, J.; Choi, B.; Cal, P. M. S. D.; Kang, S.; Kee, J.-M.; Bernardes, G. J. L.; Rohde, J.-U.; Choe, W.; Hong, S. Y. Nickel-Catalyzed Azide−Alkyne Cycloaddition To Access 1,5-Disubstituted 1,2,3-Triazoles in Air and Water. *J. Am. Chem. Soc.* **2017**, *139*, 12121−12124.

(19) Cho, I. Y.; Kim, W. G.; Jeon, J. H.; Lee, J. W.; Seo, J. K.; Seo, J.; Hong, S. Y. Nickelocene as an Air- and Moisture-Tolerant Precatalyst in the Regioselective Synthesis of Multisubstituted Pyridines. *J. Org. Chem.* **2021**, *86*, 9328−9343.

(20) Rhlee, J. H.; Maiti, S.; Lee, J. W.; Lee, H. S.; Bakhtiyorzoda, I. A.; Lee, S.; Park, J.; Kang, S. J.; Kim, Y. S.; Seo, J. K.; Myung, K.; Choe, W.; Hong, S. Y. Synthesis of α,β-Unsaturated Ketones through Nickel-Catalyzed Aldehyde-Free Hydroacylation of Alkynes. *Commun. Chem.* **2022**, *5*, 13.

(21) Jeon, J. H.; Kim, G. H.; Lee, H. S.; Kim, D. H.; Lee, S.; Choe, W.; Jung, B.; Rohde, J.-U.; Hong, S. Y. Chemo- and Regioselective Nickel-Catalyzed Reductive 1,4-Alkylarylation of 1,3-Enynes through an L_2NiAr Intermediate. *ACS Catal.* **2024**, *14*, 8996−9007.

(22) Sahoo, M. K.; Lee, J. W.; Lee, S.; Choe, W.; Jung, B.; Kwak, J.; Hong, S. Y. Isolation and Reactivity of Arylnickel(II) Complexes in Nickel-Catalyzed Borylation of Aryl Fluorosulfates. *JACS Au* **2024**, *4*, 1646−1653.

(23) Kim, G. H.; Jeon, J. H.; Jung, B.; Rohde, J.-U.; Hong, S. Y. Regioselective Transformations of Unsaturated Systems Catalyzed by Low-Valent Nickel: Cycloaddition, Hydrosilylation, and Dicarbofunctionalization. *Synlett* **2025**, *36*, 1889−1899.

(24) Hall, D. G.*Boronic Acids: Preparation and Applications in Organic Synthesis, Medicine and Materials*; Wiley-VCH: Weinheim, 2011.

(25) Lennox, A. J.; Lloyd-Jones, G. C. Selection of Boron Reagents for Suzuki−Miyaura Coupling. *Chem. Soc. Rev.* **2014**, *43*, 412−443.

(26) Brown, H. C.; Gupta, S. Hydroboration. XXXIX. 1,3,2-Benzodioxaborole (Catecholborane) as a New Hydroboration Reagent for Alkenes and Alkynes. General Synthesis of Alkane- and Alkeneboronic Acids and Esters via Hydroboration. Directive Effects in the Hydroboration of Alkenes and Alkynes with Catecholborane. *J. Am. Chem. Soc.* **1975**, *97*, 5249−5255.

(27) Tucker, C. E.; Davidson, J.; Knochel, P. Mild and Stereoselective Hydroborations of Functionalized Alkynes and Alkenes Using Pinacolborane. *J. Org. Chem.* **1992**, *57*, 3482−3485.

(28) Pereira, S.; Srebnik, M. Hydroboration of Alkynes with Pinacolborane Catalyzed by $HZrCp_2Cl$. *Organometallics* **1995**, *14*, 3127−3128.

(29) Rej, S.; Das, A.; Panda, T. K. Overview of Regioselective and Stereoselective Catalytic Hydroboration of Alkynes. *Adv. Synth. Catal.* **2021**, *363*, 4818−4840.
(30) Das, A.; Panda, T. K. Metal-Free Catalytic Hydroboration of Unsaturated Compounds: A Greener Strategy for the Synthesis of Organoboranes. *ChemCatChem.* **2023**, *15*, No. e202201011.
(31) Obligacion, J. V.; Neely, J. M.; Yazdani, A. N.; Pappas, I.; Chirik, P. J. Cobalt-Catalyzed *Z*-Selective Hydroboration of Terminal Alkynes and Elucidation of the Origin of Selectivity. *J. Am. Chem. Soc.* **2015**, *137*, 5855−5858.
(32) Yoshida, H. Borylation of Alkynes under Base/Coinage Metal Catalysis: Some Recent Developments. *ACS Catal.* **2016**, *6*, 1799−1811.
(33) Jang, H.; Zhugralin, A. R.; Lee, Y.; Hoveyda, A. H. Highly Selective Methods for Synthesis of Internal (α-)Vinylboronates through Efficient NHC−Cu-Catalyzed Hydroboration of Terminal Alkynes. Utility in Chemical Synthesis and Mechanistic Basis for Selectivity. *J. Am. Chem. Soc.* **2011**, *133*, 7859−7871.
(34) Tsuji, Y.; Fujihara, T. Copper-Catalyzed Transformations Using Cu−H, Cu−B, and Cu−Si as Active Catalyst Species. *Chem. Rec.* **2016**, *16*, 2294−2313.
(35) Gao, Y.; Yazdani, S.; Kendrick, A., IV; Junor, G. P.; Kang, T.; Grotjahn, D. B.; Bertrand, G.; Jazzar, R.; Engle, K. M. Cyclic (Alkyl)(amino)carbene Ligands Enable Cu-Catalyzed Markovnikov Protoboration and Protosilylation of Terminal Alkynes: A Versatile Portal to Functionalized Alkenes. *Angew. Chem., Int. Ed.* **2021**, *60*, 19871−19878.
(36) Yoshida, H.; Takemoto, Y.; Takaki, K. A Masked Diboron in Cu-Catalyzed Borylation Reaction: Highly Regioselective Formal Hydroboration of Alkynes for Synthesis of Branched Alkenylborons. *Chem. Commun.* **2014**, *50*, 8299−8302.
(37) Tsushima, T.; Tanaka, H.; Nakanishi, K.; Nakamoto, M.; Yoshida, H. Origins of Internal Regioselectivity in Copper-Catalyzed Borylation of Terminal Alkynes. *ACS Catal.* **2021**, *11*, 14381−14387.
(38) Li, B.; Liang, H.; Vignesh, A.; Zhou, X.; Liu, Y.; Ke, Z. Updated Progress of the Copper-Catalyzed Borylative Functionalization of Unsaturated Molecules. *Molecules* **2023**, *28*, 2252.
(39) Hwang, H. S.; Cho, E. J. Regioselective Cobalt-Catalyzed Protoboration of Alkynes. *Adv. Synth. Catal.* **2025**, *367*, No. e202401334.
(40) Zhou, M.-J.; Xu, K.; Gu, Y.; Xie, Y. Metal-Free Divergent Hydroboration/Multiboration of Terminal Alkynes via Markovnikov Pathway. *Angew. Chem., Int. Ed.* **2025**, No. e202506968.
(41) Wang, P.; Douair, I.; Zhao, Y.; Ge, R.; Wang, J.; Wang, S.; Maron, L.; Zhu, C. Selective Hydroboration of Terminal Alkynes Catalyzed by Heterometallic Clusters with Uranium−Metal Triple Bonds. *Chem.* **2022**, *8*, 1361−1375.
(42) Blasius, C. K.; Vasilenko, V.; Matveeva, R.; Wadepohl, H.; Gade, L. H. Reaction Pathways and Redox States in α-Selective Cobalt-Catalyzed Hydroborations of Alkynes. *Angew. Chem., Int. Ed.* **2020**, *59*, 23210−23214.
(43) Chen, J.; Shen, X.; Lu, Z. Cobalt-Catalyzed Markovnikov-Type Selective Hydroboration of Terminal Alkynes. *Angew. Chem., Int. Ed.* **2021**, *60*, 690−694.
(44) Ye, Z.; Ying, J.; Zhang, X.; Zhang, X.; Lu, Z. Highly Efficient and Markovnikov-Selective Cobalt Catalysis for the Construction of α-Alkenylboronates. *ACS Catal.* **2025**, *15*, 14268−14278.
(45) Chen, J.; Wei, W. T.; Li, Z.; Lu, Z. Metal-Catalyzed Markovnikov-Type Selective Hydrofunctionalization of Terminal Alkynes. *Chem. Soc. Rev.* **2024**, *53*, 7566−7589.
(46) Li, Y.; Zhang, X.; Liang, D.; Li, Y.; Gao, S.; Li, X.; Dong, Y.; Wang, B.; Ma, Y. Tunable Redox-Neutral Photocatalysis: Visible Light-Induced Arylperfluoroalkylation of Alkenes Regulated by Protons. *Asian J. Org. Chem.* **2021**, *10*, 642−648.
(47) Tang, S.; Liu, Y.; Gao, X.; Wang, P.; Huang, P.; Lei, A. Multi-Metal-Catalyzed Oxidative Radical Alkynylation with Terminal Alkynes: A New Strategy for C(sp3)−C(sp) Bond Formation. *J. Am. Chem. Soc.* **2018**, *140*, 6006−6013.
(48) Tian, H.; Yang, S.; Wang, X.; Xu, W.; Liu, Y.; Li, Y.; Wang, Q. Dehalogenative Cross-Coupling of gem-Difluoroalkenes with Alkyl Halides via a Silyl Radical−Mediated Process. *J. Org. Chem.* **2021**, *86*, 12772−12782.
(49) Li, R.; Yuan, D.; Ping, M.; Zhu, Y.; Ni, S.; Li, M.; Wen, L.; Zhang, L.-B. Electrochemically Promoted Synthesis of Benzo[b]-thiophene-1,1-dioxides via Strained Quaternary Spirocyclization. *Chem. Sci.* **2022**, *13*, 9940−9946.
(50) Mindiola, D. J.; Waterman, R.; Jenkins, D. M.; Hillhouse, G. L. Synthesis of 1,2-Bis(di-tert-butylphosphino)ethane (dtbpe) Complexes of Nickel: Radical Coupling and Reduction Reactions Promoted by the Nickel(I) Dimer [(dtbpe)NiCl]2. *Inorg. Chim. Acta* **2003**, *345*, 299−308.
(51) Ma, Z.; Mahmudov, K. T.; Aliyeva, V. A.; Gurbanov, A. V.; Pombeiro, A. J. TEMPO in Metal Complex Catalysis. *Coord. Chem. Rev.* **2020**, *423*, No. 213482.
(52) Schley, N. D.; Fu, G. C. Nickel-Catalyzed Negishi Arylations of Propargylic Bromides: A Mechanistic Investigation. *J. Am. Chem. Soc.* **2014**, *136*, 16588−16593.
(53) Ciszewski, J. T.; Mikhaylov, D. Y.; Holin, K. V.; Kadirov, M. K.; Budnikova, Y. H.; Sinyashin, O.; Vicic, D. A. Redox Trends in Terpyridine Nickel Complexes. *Inorg. Chem.* **2011**, *50*, 8630−8635.
(54) Jones, G. D.; Martin, J. L.; McFarland, C.; Allen, O. R.; Hall, R. E.; Haley, A. D.; Brandon, R. J.; Konovalova, T.; Desrochers, P. J.; Pulay, P.; Vicic, D. A. Ligand Redox Effects in the Synthesis, Electronic Structure, and Reactivity of an Alkyl−Alkyl Cross-Coupling Catalyst. *J. Am. Chem. Soc.* **2006**, *128*, 13175−13183.
(55) Bhattacharjee, J.; Harinath, A.; Bano, K.; Panda, T. K. Highly Chemoselective Hydroboration of Alkynes and Nitriles Catalyzed by Group 4 Metal Amidophosphine−Borane Complexes. *ACS Omega* **2020**, *5*, 1595−1606.
(56) He, X.; Hartwig, J. F. True Metal-Catalyzed Hydroboration with Titanium. *J. Am. Chem. Soc.* **1996**, *118*, 1696−1702.
(57) Zhang, G.; Li, S.; Wu, J.; Zeng, H.; Mo, Z.; Davis, K.; Zheng, S. Highly Efficient and Selective Hydroboration of Terminal and Internal Alkynes Catalyzed by a Cobalt(II) Coordination Polymer. *Org. Chem. Front.* **2019**, *6*, 3228−3233.
(58) Zobernig, D. P.; Stöger, B.; Veiros, L. F.; Kirchner, K. Hydroboration of Terminal Alkynes Catalyzed by a Mn(I) Alkyl PCP Pincer Complex Following Two Diverging Pathways. *ACS Catal.* **2024**, *14*, 12385−12391.
(59) Johnson, E. R.; Keinan, S.; Mori-Sánchez, P.; Contreras-García, J.; Cohen, A. J.; Yang, W. Revealing Noncovalent Interactions. *J. Am. Chem. Soc.* **2010**, *132*, 6498−6506.
(60) Dennington, R.; Keith, T.; Millam, J.*GaussView, version 5.0.9*; Semichem, Inc.: Shawnee Mission, KS, **2009**.
(61) Humphrey, W.; Dalke, A.; Schulten, K. VMD: Visual Molecular Dynamics. *J. Mol. Graph.* **1996**, *14*, 33-38−27-28.
(62) Chen, J.; Wei, H.; Gridnev, I. D.; Zhang, W. Weak Attractive Noncovalent Interactions in Metal-Catalyzed Asymmetric Hydrogenation. *Angew. Chem., Int. Ed.* **2025**, No. e202425589.
(63) Lu, G.; Liu, R. Y.; Yang, Y.; Fang, C.; Lambrecht, D. S.; Buchwald, S. L.; Liu, P. Ligand−Substrate Dispersion Facilitates the Copper-Catalyzed Hydroamination of Unactivated Olefins. *J. Am. Chem. Soc.* **2017**, *139*, 16548−16555.
(64) Toste, F. D.; Sigman, M. S.; Miller, S. J. Pursuit of Noncovalent Interactions for Strategic Site-Selective Catalysis. *Acc. Chem. Res.* **2017**, *50*, 609−615.
(65) Davis, H. J.; Phipps, R. J. Harnessing Noncovalent Interactions to Exert Control over Regioselectivity and Site-Selectivity in Catalytic Reactions. *Chem. Sci.* **2017**, *8*, 864−877.

https://doi.org/10.1021/acscatal.6c00028
ACS Catal. 2026, 16, 7551−7561